Journal of Electromagnetic Waves and Applications, Vol. 1, No. 4, 377–402, 1987

Exact Solution of the Sommerfeld Half-Plane Problem: a Path Integral Approach Without Discretization

R. W. Ziolkowski

Lawrence Livermore National Laboratory
P. O. Box 5504, L-156
Livermore, CA 94550, USA

Abstract- The exact solution of the two-dimensional Sommerfeld half-plane problem is obtained with a path integral approach. The approach relies on the Riemann space associated with this problem but does not require discretization nor a transformation to the corresponding heat conduction problem. A new intrinsic symmetry property of the half-plane problem solutions is revealed and is connected to the characteristics of the underlying Riemann space. An endpoint rather than a stationary point argument reproduces Keller's GTD results from the path integral expression.

1. INTRODUCTION

The similarity of quantum mechanics and electromagnetics results from the wave nature of the phenomena they both attempt to describe. The Feynman Path Integral (FPI) represents in a particular manner the interference effects of quantum mechanics. A similar path integral representation should also be capable of describing the interference of electromagnetic waves.

Imitating Feynman's reasoning [1], a solution of the scalar Helmholtz equation in two dimensions:

$$\{\Delta + k^2\}K(\vec{r},\vec{r}_0) = \delta(\vec{r}-\vec{r}_0) \tag{1.1}$$

can be represented in path integral (PI) form as

$$K(\vec{r},\vec{r}_0) = \int_\Gamma e^{\nu(S|\gamma)}\, D\gamma \tag{1.2}$$

where $\nu = ik$ and where $\exp[\nu(S|\gamma)]$ is the value assigned to the path γ which connects the source point $\vec{r}_0 = (r_0,\theta_0)$ to the observation point $\vec{r} = (r,\theta)$. The set Γ represents all possible γ. The classical action, $(S|\gamma)$, along γ is the optical length of γ:

$$S|\gamma = \int_\gamma n\, d\ell \tag{1.3}$$

where ℓ is the arc-length parameter and n is the index of refraction of the

medium. The path integral (1.2) is viewed as describing an interference effect between the paths in Γ.

There are two major difficulties encountered in the evaluation of the representation (1.2). First, in contrast to the Wiener integral, a procedure to calculate the measure $D\gamma$ in (1.2) is not known. Secondly, in contrast to the Schrödinger equation (for which the FPI was derived), there is no preferred coordinate associated with the reduced wave equation. The present problem requires an enlarged path set. In particular, paths that intersect with themselves and that traverse coordinate planes any number of times (a path set with a preferred time coordinate would contain paths that cross a spatial coordinate plane only in one direction) are now allowed. Thus, the standard discretization process, which is based on a preferred coordinate, is not applicable.

A path integral interpretation of the free-space solution of (1.1):

$$K_F(\vec{r},\vec{r}_0) = \frac{i}{4}H_0^{(1)}(ks_0) \tag{1.4}$$

where $s_0 = |\vec{r} - \vec{r}_0|$ is the straight line distance between $\vec{r}_0$ and $\vec{r}$, is developed in Section 2. It has the form (1.2) and is based on a decomposition of the path set Γ into sets of paths whose elements share equal path-lengths. As in Ziolkowski [2], a Riemann space is introduced in Section 3 to represent the boundary conditions imposed by the diffracting half-plane. The modification of the free-space path-length set by the presence of the half-plane is then easily explained. The PI on this two-sheeted covering of the physical space follows readily. The actual half-plane solution is constructed in Section 4 and is shown to be exact. Keller's [3] GTD results are trivially reproduced in Section 5 from the PI solution. However, in contrast to the usual PI asymptotic analyses based upon stationary phase concepts, an endpoint evaluation of the expressions is employed. Finally, an equivalent detour representation of the half-plane solution is developed in parallel with the path-length description. In Section 6 it is used to reveal a new symmetry relation characteristic of the half-plane solutions. This relation is linked to the properties of the underlying Riemann space and an associated inhomogeneous Riemann-Hilbert problem [4]. Various ramifications of this symmetry property are discussed.

Several other PI approaches to half-plane problems have appeared recently in the literature. In contrast to Lee [5] and Ziolkowski [2], the original electromagnetics problem is *not* converted to an equivalent heat problem. Moreover, in [5] the results are restricted to the case where the observation point is located exactly on the incident shadow boundary and to only the leading term of order k^0 in the asymptotic field solution. As noted above, the *exact* solution (everywhere) is derived in this paper. In contrast with Schulman [6] (upon which [7] is based) and Lee [5], a semigroup property argument is not employed. Thus, necessary assumptions about particular intermediate time parameters are avoided. However, in analogy with [5-7], the modification of the path set by the presence of the half-plane is shown to be responsible for reproducing the diffraction effects. Several aspects of the derivation in Section 3 are quite similar conceptually with

the approach taken by Wiegel and Boersma[8] in solving the corresponding heat conduction problem. Solutions of the corresponding wedge problems based on path integral techniques on multiply-connected spaces have been discussed by Dowker[9], DeWitt-Morette *et al* [10], Crandall[11], and Ziolkowski[2].

2. PATH INTEGRAL INTERPRETATION OF THE FREE-SPACE PROPAGATOR

Consider the free-space propagator (1.4). A simple manipulation of the expression [12, 8.42.11] yields the equivalent representation:

$$K_F(\vec{r},\vec{r}_0) = \frac{1}{2\pi}\int_{s_0}^{\infty} \frac{e^{\nu s}\,ds}{(s^2 - s_0^2)^{1/2}} \tag{2.1}$$

Starting with (1.2), a PI interpretation of (2.1) is given in this section. This identification is facilitated with the following decomposition of the path set Γ.

2.1 Path-Length Representation

Since the index of refraction $n = 1$ in free-space, the term $S|\gamma$ appearing in (1.2) reduces simply to s, the path length of γ. Consequently, let the path set Γ, which is composed of all of the paths connecting $\vec{r}_0$ to $\vec{r}$, be decomposed into disjoint subsets, Γ_s, which consist of all those paths in Γ whose path length is s; i.e., let

$$\Gamma_s = \{\text{all } \gamma \in \Gamma \,\Big|\, (S|\gamma) = s\} \tag{2.2a}$$

so that

$$\Gamma_s \cap \Gamma_t = 0 \qquad \text{if} \quad s \neq t \tag{2.2b}$$

and

$$\Gamma = \bigcup_{s_1 \le s \le s_2} \Gamma_s \tag{2.2c}$$

where s_1 and s_2 are, respectively, the minimum and maximum path lengths attained by any path in Γ. This classification of the paths simplifies the analysis of the PI (1.2) since the subsets, Γ_s, are characterized by one fundamental parameter. Moreover, because the value assigned to a path in (1.2) now depends only on its path length, all the paths in a particular subset Γ_s contribute to the propagator with the same strength. Therefore, one can concentrate on the contributions to the propagator of the individual subsets Γ_s rather than examining the influence of each γ in Γ.

This path-length decomposition then allows one to express the PI (1.2) as

$$K(\vec{r},\vec{r}_0) = \int_\Lambda e^{\nu s} \int_{\Gamma_s} D\gamma = \int_\Lambda \alpha(\Gamma_s)\,ds \tag{2.3}$$

where the value assigned to the path set Γ_s is

$$\alpha(\Gamma_s) = e^{\nu s} A(\vec{r}, \vec{r}_0; s) \tag{2.4}$$

and where Λ denotes the interval in R that represents the set of possible (distinct) path lengths of the paths in Γ: $\Lambda = [s_1, s_2]$. The path-length set Λ is determined solely by the scattering geometry. Notice that the interference viewpoint remains intact in (2.3), but now there is an additional amplitude factor, $A(\vec{r}, \vec{r}_0; s)$, which represents the collective effects of the paths in Γ_s and is related to a measure of the size of that subset:

$$A(\vec{r}, \vec{r}_0; s) = \int_{\Gamma_s} D\mu \tag{2.5}$$

where $D\gamma = D\mu\, ds$.

The geometry of the free-space problem is illustrated in Fig. 1. It is obvious that the path-length set $\Lambda_F = [s_0, \infty[$. Therefore the free-space amplitude factor associated with Γ_s is obtained immediately from (2.1):

$$A_F(\vec{r}, \vec{r}_0; s) = \frac{1}{2\pi(s^2 - s_0^2)^{1/2}} \tag{2.6}$$

A heuristic derivation of this term follows.

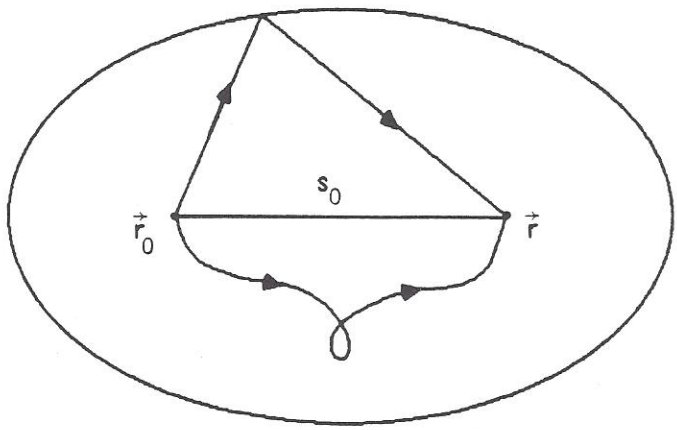

Figure 1. Paths of length s sweep out an ellipse of area $\frac{\pi}{4}s(s^2 - s_0^2)^{1/2}$.

Consider the path set Γ_s. A path in Γ_s can be visualized as an *arbitrary* configuration of a (continuous) string of length s connecting $\vec{r}_0$ to $\vec{r}$. As shown in Fig. 1, the paths in Γ_s sweep out the area of the ellipse whose foci are located at $\vec{r}_0$ and $\vec{r}$. This planar area is $a(s, s_0) = \frac{\pi}{4}s(s^2 - s_0^2)^{1/2}$. The associated quantity $a(s, s_0)/s \equiv N(s, s_0)$, the area per path length s, can be viewed as a

measure of the number of paths in Γ_s. However, with respect to the propagator (2.3), (2.5) not only measures the extent of Γ_s, it also reflects the collective importance of its elements to the overall description of the physics. Drawing from standard asymptotic analyses, one observes that for k large in (2.3), the paths whose length s is closest to the minimum path-length will contribute the most to the propagator. Consequently, the description of the physical system should be *biased* to give more importance to those paths. Longer length paths should make a relatively smaller contribution to the propagator; hence, they should have a smaller "physical" measure. On the other hand, paths of smaller lengths are less numerous: if $s < t$, then $N(s, s_0) < N(t, s_0)$. Therefore, the amplitude factor $A_F(\vec{r}, \vec{r}_0; s)$ is set proportional to the inverse of $N(s, s_0)$:

$$A_F(\vec{r}, \vec{r}_0; s) = c(s^2 - s_0^2)^{-1/2}$$

to reflect the "biased measure" concept. This assignment clearly gives $A_F(\vec{r}, \vec{r}_0; s) > A_F(\vec{r}, \vec{r}_0; t)$ if $t > s$. The boundary conditions for the propagator fix the normalization constant to be $c = 1/2\pi$; and hence, the amplitude (2.6) is recovered.

From this free-space result I deduce that for a general scattering problem in which the space of interest is almost everywhere R^2, the propagator (2.3) takes the form:

$$K(\vec{r}, \vec{r}_0) = \frac{1}{2\pi} \int_{s_1}^{s_2} \frac{e^{\nu s}\, ds}{(s^2 - s_0^2)^{1/2}} \tag{2.7}$$

The allowed paths, hence, the endpoints, s_1 and s_2, of the path-length set Λ are then determined by the physics of the problem.

At first glance, this "biased measure" concept may seem incompatible with Feynman's PI construction. It is not. As demonstrated, for example, in [1], the major contributions to a PI result from the paths that minimize the action. In the present context, those paths are the ones of minimum length. Moreover, the path set decomposition approach and the associated formation of a measure which embraces the resulting collective effects also rely heavily on the physics of the problem. This approach simply reduces the PI to a more tractable form.

2.2 Detour Parameter Representation

A physically appealing representation of the expression (2.7) is generated with the following change of variables. Let

$$\tau = [k(s - s_0)]^{1/2} \tag{2.8}$$

so that $s = (\tau^2/k) + s_0$ and $ds = (2\tau/k)d\tau$. Since $k(s - s_0)$ is a measure of the difference in phase of the paths γ and γ_0 whose path lengths are, respectively, s and s_0, the parameter τ describes the amount of deviation or detour of the path γ from γ_0. Hence, it is called the *detour parameter*. Intuitively, a parameter such as τ should play a major role in the analysis of diffraction problems. It has appeared already in this context in [13].

The equivalent detour parameter representation of the propagator (2.7) is

$$K(\vec{r},\vec{r}_0) = \int_T \tilde{\alpha}(\Gamma_\tau)\, d\tau = \frac{e^{\nu s_0}}{\pi} \int_{\tau_1}^{\tau_2} \frac{e^{i\tau^2}\, d\tau}{(\tau^2 + 2ks_0)^{1/2}} \tag{2.9}$$

where $\tau_i = [k(s_i - s_0)]^{1/2}$ for $i = 1,2$ such that the detour parameter set $T = [\tau_1, \tau_2]$. This expression represents a weighted Gaussian distribution with a complex variance. Thus, the PI solution can be reduced either to an analysis of the paths in terms of their path lengths or their detour parameters. Notice that the free-space propagator (2.1) becomes

$$K_F(\vec{r},\vec{r}_0) = \frac{e^{\nu s_0}}{\pi} \int_0^\infty \frac{e^{i\tau^2}\, d\tau}{(\tau^2 + 2ks_0)^{1/2}} = \frac{e^{\nu s_0}}{2\pi} \int_{-\infty}^\infty \frac{e^{i\tau^2}\, d\tau}{(\tau^2 + 2ks_0)^{1/2}} \tag{2.1'}$$

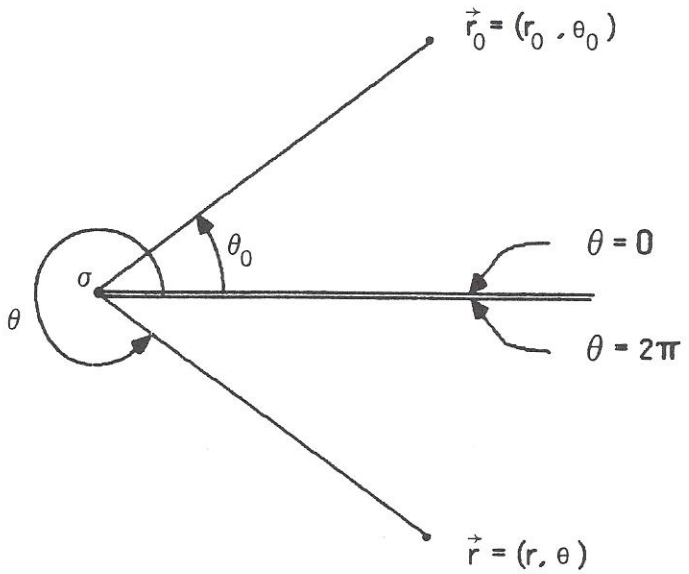

Figure 2. The geometry of the half-plane problem employs a cylindrical coordinate system.

3. P_2-SPACE PATH INTEGRAL

The geometry of the Sommerfeld problem is shown in Fig. 2. Cartesian coordinate (x,y,z) and cylindrical coordinate (r,θ,z) systems are erected at the edge of a perfectly conducting half-plane. The z-axis coincides with its edge; the $\theta = 0$ and positive x-axis lie along the half-plane. Positive angles are measured in a counterclockwise direction. The physical space $[0,\infty[\times [0,2\pi]$ is denoted by P. A line source parallel to the edge is located at $\vec{r}_0 = (r_0,\theta_0)$. This assumption reduces the three-dimensional vector problem to a two-dimensional

scalar problem. The observation point is $\vec{r} = (r, \theta)$. A solution $U(\vec{r})$ of (1.1) is sought that, depending on the given polarization of the incident wave, satisfies on the half-plane either of the boundary conditions:
(1) the solution $U(\vec{r}) = 0$ [electric field parallel to the edge] (3.1*a*)
(2) the normal derivative $\partial_n U(\vec{r}) = 0$ [magnetic field parallel to the edge] (3.1*b*)
and that satisfies the radiation condition at infinity.

3.1 Riemann Space P_2

Following Sommerfeld [14] and Ziolkowski [2], the original diffraction problem in the physical space P is converted to one in a space P_2 constructed as follows. Take two replicas of P, called P_+ and P_-, and join them along the half-plane, Σ. Then

$$P_2 = P_+ \cup P_- \cup \Sigma$$

The spaces P_+ and P_- will be respectively called the upper and lower sheets of P_2; the space P_+ is identified with the physical space P. To suggest pictorally the two sheets, the "edge" of P_- is drawn outside that of P_+ as shown in Fig. 3.

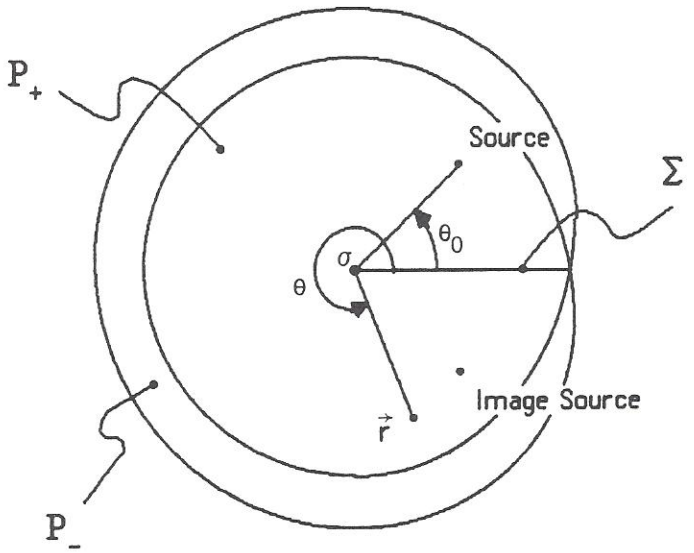

Figure 3. The introduction of the P_2-space, a two-sheeted surface, removes the half-plane boundary.

The space P_2 is the Riemann space associated with the half-plane problem and coincides with the one introduced by Sommerfeld [14]. Natural coordinates in P_2 are the distance r from the origin and the polar angle θ measured from the upper edge ($\theta = 0$) of the half-plane. This angle now varies from 0 to 4π.

The angles $\theta = 0$ and $\theta = 2\pi$ have no special properties. In fact, the ef-

fect of introducing P_2 may be considered as "erasing" the boundaries, Σ. The boundary conditions (3.1) are satisfied by locating an image source on P_- at $\vec{r}_0{}' = (r_0, -\theta_0)$. The desired field can be decomposed as

$$U(\vec{r}) = K(\vec{r}, \vec{r}_0) \mp K(\vec{r}, \vec{r}_0{}') \tag{3.2}$$

the minus [plus] sign solution satisfying (3.1a) [(3.1b)]. The P_2-space propagators $K(\vec{r}, \vec{r}_0)$ and $K(\vec{r}, \vec{r}_0{}')$ represent, respectively, the field at $\vec{r}$ due to the sources at $\vec{r}_0$ and $\vec{r}_0{}'$. Their construction is a main object of this paper and will be considered next.

3.2 Path Integral on P_2

The propagators $K(\vec{r}, \vec{r}_0)$ and $K(\vec{r}, \vec{r}_0{}')$ will be generated with the path-length decomposition introduced in Section 2. However, because the edge of the half-plane is a singular point, one must now also account for topologically inequivalent path sets. In particular, let p be the map that projects P_2 onto P. It maps the two preimages (r, θ) in P_+ and $(r, \theta + 2\pi)$ in P_- onto $\vec{r}$ in P. Let $\phi[\gamma, \sigma]$ be the angle swept out by a path γ with respect to the edge, $\sigma = \vec{0}$, of the half-plane and measured from the $\theta = 0$ axis [15, Sec. 20]. Then with [Thm. 22.1, 15] one has for a path ξ in P_2 connecting $\vec{r}_0$ to $\vec{r}$:

$$\phi[p(\xi), \sigma] = \theta - \theta_0 + m\, 2\pi \tag{3.3a}$$

where m is an integer. Similarly, for a path ζ in P_2 connecting $\vec{r}_0{}'$ to $\vec{r}$:

$$\phi[p(\zeta), \sigma] = \theta + \theta_0 + m\, 2\pi \tag{3.3b}$$

Any path associated with the propagator $K(\vec{r}, \vec{r}_0)$ or $K(\vec{r}, \vec{r}_0{}')$ must, respectively, be either of the ξ or the ζ type. The allowed values of m in both cases depend on the relative locations of $\vec{r}_0$, $\vec{r}_0{}'$, and $\vec{r}$ on P_+ and P_-. In particular, for the ξ-paths one finds that m can only take the values $\{\cdots, -5, -3, -1, 0, +2, +4, +6, \cdots\} \equiv I_>$, when $\theta \geq \theta_0$; and the values $\{\cdots, -6, -4, -2, 0, +1, +3, +5, \cdots\} \equiv I_<$, when $\theta < \theta_0$. For instance, when $\theta \geq \theta_0$, the observation point $\vec{r}$ can be reached from the source point $\vec{r}_0$ by either (a) leaving $\vec{r}_0$ and encircling σ in a positive (counterclockwise) sense $2n$ times before reaching $\vec{r}$ or (b) leaving $\vec{r}_0$ and encircling σ in a negative (clockwise) sense $2n+1$ times before reaching $\vec{r}$. The first type of excursion gives the nonnegative values in $I_>$, the second gives the negative values. Examples of configurations having paths with edge interaction indexes in $I_>$ and in $I_<$ are given respectively in Figs. 4a and 4b. Note that the value of $\phi(p(\xi), \sigma)/2\pi$ rounded down to the nearest integer can be interpreted as the *winding number* of ξ with respect to σ; i.e., the number of times ξ completely encircles or "winds around" σ. Clearly, if $\theta < \theta_0$, then the winding number of a ξ-path with respect to σ is always one less then it would be if $\theta > \theta_0$. This explains why $I_< = I_> - 1$. Similarly, for the ζ-paths the factor $m \in I_>$ when $p(4\pi - \theta_0) > p(\theta)$ and $m \in I_<$ when $p(4\pi - \theta_0) < p(\theta)$. Examples of these configurations are given respectively in Figs. 4c and 4d.

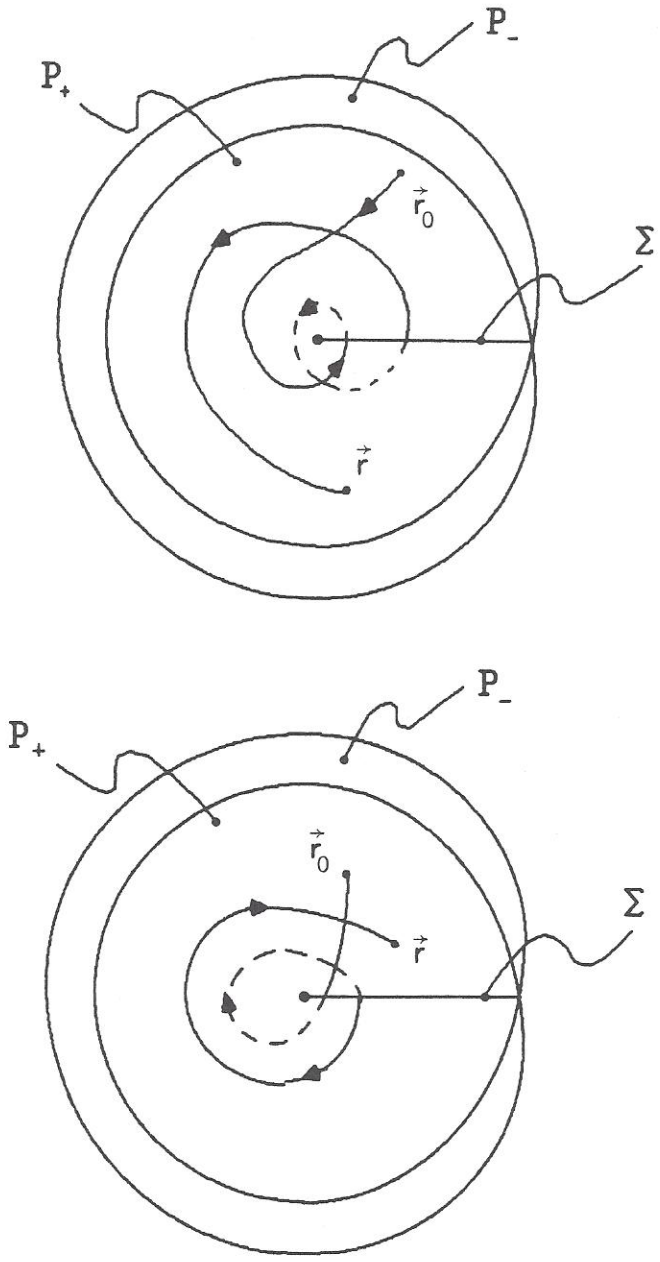

Figure 4. See caption on Page 386.

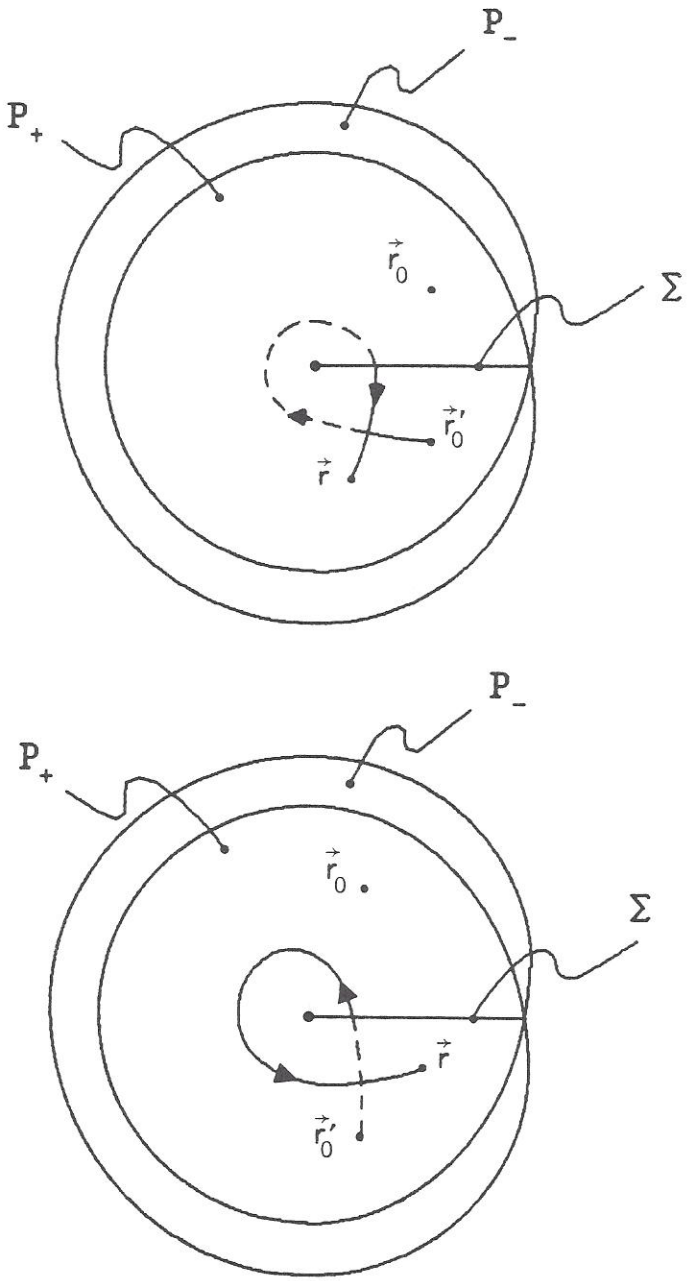

Figure 4. Different source-edge-observation point configurations lead to different allowed values of m in Eqs. (3.3a) and (3.3b): (a) $\theta > \theta_0$ and $m = +2$; (b) $\theta < \theta_0$ and $m = -2$; (c) $p(4\pi - \theta_0) > p(\theta)$ and $m = -1$; and (d) $p(4\pi - \theta_0) < p(\theta)$ and $m = +1$.

Referring to (3.3*a*) and (3.3*b*), I define the *edge interaction index* of a path γ to be

$$n_\sigma(\gamma) = |m| \tag{3.4}$$

It is a nonnegative integer for any path of the ξ or ζ type. The edge interaction index is a measure of the number of times a path wraps around the edge of the half-plane.

Consider the path set Γ associated with the propagator $K(\vec{r},\vec{r}_0)$. It can be decomposed into the topologically inequivalent path sets $\Gamma_0,\Gamma_1,\Gamma_2,\cdots$ characterized by the edge interaction index; e.g., Γ_1 represents all paths $\gamma \in \Gamma$ with $n_\sigma(\gamma) = 1$. Each Γ_m ($m = 0,1,2,\cdots$) can then be decomposed further into equal path-length subsets and the associated path-length sets Λ_m can be determined. The corresponding amplitude factors coincide with the free-space term (2.6). This simplification arises because the P_2-space construction has not altered the path-length measure; the space P_2 is simply fabricated from two replicas of P, free-space. Therefore, the contribution to the propagator $K(\vec{r},\vec{r}_0)$ from each of the topologically distinct path subsets Γ_m takes the form of (2.7):

$$K_m(\vec{r},\vec{r}_0) = \frac{1}{2\pi}\int_{\Lambda_m} \frac{e^{\nu s}\,ds}{(s^2 - s_0^2)^{1/2}} \tag{3.5}$$

For the diffraction problem, the paths of length s that are in Γ_m will not be the same as those in Γ_s for the free-space case because of the presence of the diffracting edge. This modification of the allowed paths will be seen to be responsible for the diffraction effects.

Following standard prescriptions [2, 8-11, 16-20], the contributions from each of the topologically distinct path subsets must be added with relative phase terms $\chi(\Gamma_m)$ to yield the total propagator

$$K(\vec{r},\vec{r}_0) = \sum_{m=0}^{\infty} \chi(\Gamma_m)\, K_m(\vec{r},\vec{r}_0) \tag{3.6}$$

This representation is a manifestation of the multi-valuedness of the propagator on P_2. The terms $\chi(\Gamma_m)$ are necessarily a unitary, one-dimensional representation of the fundamental group of the covering space of P_2. Because P_2 is a double covering of P, the phase factors are thus simply

$$\chi(\Gamma_m) = e^{im\pi} \tag{3.7}$$

so that $|\chi(\Gamma_m)| = 1$ and $\chi(\Gamma_m)\chi(\Gamma_n) = \chi(\Gamma_{m+n})$. The contributions to (3.6) from all even or all odd edge interaction numbered paths therefore add in phase, but the even and odd sets add completely out of phase. The equivalence of the paths with either an even or an odd interaction index is expected because a closed path on P_2, which will return a function to its original value [see, for instance,

(6.14) below], has an angular extent of $n4\pi$, hence, an edge interaction index of $2n$. The $+1$ weight to the "even" path sets and -1 weight to the "odd" ones is also expected because the group that is naturally associated with solutions based on P_2 is the monodromy group $\{e^{in\pi}; n = 0, 1\}$. This property reflects the fact that the edge σ is the location of a square root branch point.

The paths in all of the sets Γ_m $(m = 1, 2, \ldots)$ will be called *indirect paths* because they must first "interact" with the edge before reaching the observation point. The minimum length indirect path for each index value is the same. It is the piecewise straight path $\vec{r}_0\sigma\vec{r}$ whose length is $r_0 + r$. In contrast, the paths in Γ_0 will be called *direct paths*. The minimum length of a direct path, s_{min}, is determined by the relative configuration of $\vec{r}_0$, σ, and $\vec{r}$. Paths with infinite length are the maximum for all index subsets. Thus, the path-length sets $\Lambda_0 = [s_{min}, \infty[\equiv \Lambda_d$ and $\Lambda_m = [r_0 + r, \infty[\equiv \Lambda_i$ for $m = 1, 2, \ldots$. This reduces the real source propagator (3.6) to a sum of the contributions from the direct and the indirect paths:

$$K(\vec{r}, \vec{r}_0) = K_d(\vec{r}, \vec{r}_0) + K_i(\vec{r}, \vec{r}_0) \tag{3.8}$$

Because the minimum path length for all of the indirect paths is the same, the partial propagators $K_m(\vec{r}, \vec{r}_0)$ will be identical for all $m = 1, 2, \ldots$. However, to avoid the difficulties associated with summing unit amplitude terms, I follow the standard practice of introducing into (3.6) a small decay term $e^{-m\epsilon}$, $\epsilon \ll 1$, from each of the partial propagators $K_m(\vec{r}, \vec{r}_0)$; perform the required sum; and then take the limit $\epsilon \to 0$. This yields

$$K_i(\vec{r}, \vec{r}_0) = \sum_{m=1}^{\infty} \chi(\Gamma_m) K_m(\vec{r}, \vec{r}_0) = -\frac{1}{2}\Big[\frac{1}{2\pi} \int_{\Lambda_i} \frac{e^{\nu s}\, ds}{(s^2 - s_0^2)^{1/2}}\Big] \tag{3.9}$$

Consequently, the real source propagator (3.6) becomes

$$K(\vec{r}, \vec{r}_0) = \frac{1}{2\pi} \int_{s_{min}}^{\infty} \frac{e^{\nu s}\, ds}{(s^2 - s_0^2)^{1/2}} - \frac{1}{4\pi} \int_{r+r_0}^{\infty} \frac{e^{\nu s}\, ds}{(s^2 - s_0^2)^{1/2}} \tag{3.8'}$$

Setting the detour parameters $\tau_{min} = [k(s_{min} - s_0)]^{1/2}$ and

$$\eta = [k(r + r_0 - s_0)]^{1/2} = \Big[k(r + r_0 - s_0)\, \frac{(r + r_0 + s_0)}{(r + r_0 + s_0)}\Big]^{1/2}$$

$$= (2k\rho)^{1/2} \Big|\cos\Big(\frac{\theta - \theta_0}{2}\Big)\Big| \tag{3.10}$$

where $\rho = 2rr_0/(r + r_0 + s_0)$ and explicitly $s_0 = [r^2 + r_0^2 - 2rr_0 \cos(\theta - \theta_0)]^{1/2}$, the detour parameter representation of (3.8′) is

$$K(\vec{r},\vec{r}_0) = \frac{e^{\nu s_0}}{\pi}\int_{\tau_{min}}^{\infty}\frac{e^{i\tau^2}\,d\tau}{(\tau^2+2ks_0)^{1/2}} - \frac{e^{\nu s_0}}{2\pi}\int_{\eta}^{\infty}\frac{e^{i\tau^2}\,d\tau}{(\tau^2+2ks_0)^{1/2}} \tag{3.11}$$

These propagator expressions can be simplified by introducing the functions

$$V(a,b) = \frac{1}{2\pi}\int_b^{\infty}\frac{e^{\nu s}\,ds}{(s^2-a^2)^{1/2}} \tag{3.12}$$

$$W(\alpha,\beta) = \frac{e^{\nu\alpha}}{\pi}\int_{\beta}^{\infty}\frac{e^{i\tau^2}\,d\tau}{(\tau^2+2k\alpha)^{1/2}} \tag{3.13}$$

In particular,

$$\begin{aligned} K(\vec{r},\vec{r}_0) &= V(s_0,s_{min}) - \frac{1}{2}V(s_0,r+r_0) \\ &= W(s_0,\tau_{min}) - \frac{1}{2}W(s_0,\eta) \end{aligned} \tag{3.14}$$

The important features of the direct and indirect path contributions and the essential differences between them are much more apparent in these forms. They will be utilized extensively in the following sections.

The image source propagator is obtained in a similar fashion. In particular, with $\tau'_{min} = [k(s'_{min} - s'_0)]^{1/2}$ and

$$\eta' = [k(r+r_0-s'_0)]^{1/2} = (2k\rho')^{1/2}\left|\cos\left(\frac{\theta+\theta_0}{2}\right)\right| \tag{3.10'}$$

where $\rho' = 2rr_0/(r+r_0+s'_0)$ and $s'_0 = |\vec{r}-\vec{r}_0{}'| = [r^2+r_0^2-2rr_0\cos(\theta+\theta_0)]^{1/2}$, one simply has

$$\begin{aligned} K(\vec{r},\vec{r}_0{}') &= K_d(\vec{r},\vec{r}_0{}') + K_i(\vec{r},\vec{r}_0{}') \\ &= V(s'_0,s'_{min}) - \frac{1}{2}V(s'_0,r+r_0) = W(s'_0,\tau'_{min}) - \frac{1}{2}W(s'_0,\eta') \end{aligned} \tag{3.14'}$$

4. HALF-PLANE SOLUTION

To complete the construction of the half-plane problem solution, the values s_{min} and s'_{min} of the minimum length direct paths ξ_d and ζ_d must be determined. As indicated above, they depend on the relative locations of the source and observation points and the edge of the half-plane. There are three distinct configurations. Referring to Fig. 5, they are

1. $\vec{r}$ lies in Region I, the shadow of both the actual and image sources, where $\theta \in]\pi+\theta_0, 2\pi]$

2. $\vec{r}$ lies in Region II, the lit region of the actual source and the shadow of the image source, where $\theta \in]\pi - \theta_0, \pi + \theta_0]$
3. $\vec{r}$ lies in Region III, the lit region of both the actual and image sources, where $\theta \in [0, \pi - \theta_0]$.

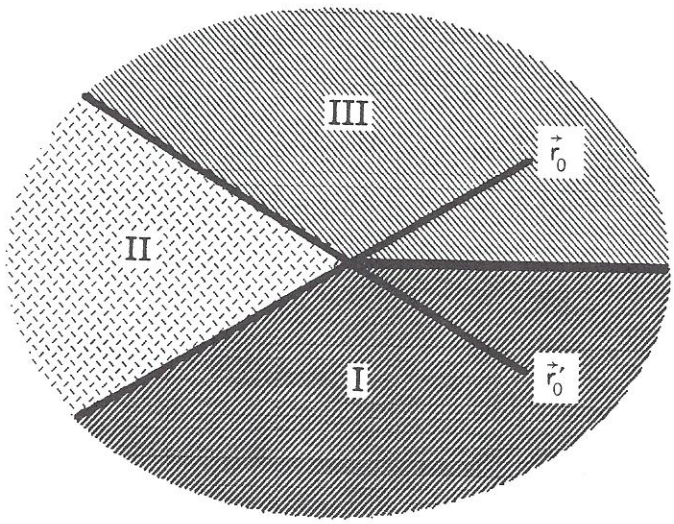

Figure 5. The shadow boundaries of the source and its image divide the space P into three distinct regions.

Consider the first case. As shown in Fig. 6a, the minimum length direct paths are the piecewise straight paths $\xi_d = \vec{r}_0\sigma\vec{r}$ and $\zeta_d = \vec{r}_0{}'\sigma\vec{r}$. Their path-lengths are both $r + r_0$. Consequently, the propagators

$$K(\vec{r}, \vec{r}_0) = V(s_0, r + r_0) - \frac{1}{2}V(s_0, r + r_0) = \frac{1}{2}V(s_0, r + r_0)$$

$$K(\vec{r}, \vec{r}_0{}') = V(s_0', r + r_0) - \frac{1}{2}V(s_0', r + r_0) = \frac{1}{2}V(s_0', r + r_0)$$

and the total field (3.2) is

$$U(\vec{r}) = \frac{1}{2}[V(s_0, r + r_0) \mp V(s_0', r + r_0)] = \frac{1}{2}[W(s_0, \eta) \mp W(s_0', \eta')] \quad (4.1)$$

Consider now the second case. As shown in Fig. 6b, the minimum length direct paths are the straight-line path $\xi_d = \vec{r}_0\vec{r}$ and the piecewise straight path $\zeta_d = \vec{r}_0{}'\sigma\vec{r}$. Their lengths are respectively s_0 and $r_0 + r$. Notice that the free-space propagator

$$K_F(\vec{r},\vec{r}_0) = V(s_0,s_0) = W(s_0,0) = \frac{1}{2}W(s_0,-\infty) \tag{4.2}$$

Consequently, the propagators

$$K(\vec{r},\vec{r}_0) = V(s_0,s_0) - \frac{1}{2}V(s_0,r+r_0) \equiv K_F(\vec{r},\vec{r}_0) - \frac{1}{2}V(s_0,r+r_0)$$

$$K(\vec{r},\vec{r}_0{}') = V(s_0',r+r_0) - \frac{1}{2}V(s_0',r+r_0) = \frac{1}{2}V(s_0',r+r_0)$$

and the total field (3.2) becomes

$$\begin{aligned} U(\vec{r}) &= K_F(\vec{r},\vec{r}_0) - \frac{1}{2}[V(s_0,r+r_0) \pm V(s_0',r+r_0)] \\ &= \frac{1}{2}[W(s_0,-\eta) \mp W(s_0',\eta')] \end{aligned} \tag{4.3}$$

The last relation required (4.2) and the identity

$$\begin{aligned} W(s_0,-\infty) - W(s_0,\eta) &= \frac{e^{\nu s_0}}{\pi}\int_{-\infty}^{\eta}\frac{e^{i\tau^2}\,d\tau}{(\tau^2+2ks_0)^{1/2}} = \frac{e^{\nu s_0}}{\pi}\int_{-\eta}^{\infty}\frac{e^{i\tau^2}\,d\tau}{(\tau^2+2ks_0)^{1/2}} \\ &= W(s_0,-\eta) \end{aligned} \tag{4.4}$$

Finally, consider the third case. As shown in Fig. 6c, the minimum length direct paths are now the straight line paths $\xi_d = \vec{r}_0\vec{r}$ and $\zeta_d = \vec{r}_0{}'\vec{r}$. Their lengths are respectively s_0 and s_0'. Consequently, the propagators

$$K(\vec{r},\vec{r}_0) = V(s_0,s_0) - \frac{1}{2}V(s_0,r+r_0) \equiv K_F(\vec{r},\vec{r}_0) - \frac{1}{2}V(s_0,r+r_0)$$

$$K(\vec{r},\vec{r}_0{}') = V(s_0',s_0') - \frac{1}{2}V(s_0',r+r_0) \equiv K_F(\vec{r},\vec{r}_0{}') - \frac{1}{2}V(s_0',r+r_0)$$

and the total field

$$\begin{aligned} U(\vec{r}) &= K_F(\vec{r},\vec{r}_0) \mp K_F(\vec{r},\vec{r}_0{}') - \frac{1}{2}[V(s_0,r+r_0) \pm V(s_0',r+r_0)] \\ &= \frac{1}{2}[W(s_0,-\eta) \mp W(s_0',-\eta')] \end{aligned} \tag{4.5}$$

Comparing the expressions (4.1), (4.3), and (4.5) with those given in [21, Section 11.7], it is verified immediately that the exact solution has been recovered in all cases. Such comparisons are facilitated by deriving a single expression that encompasses all three cases.

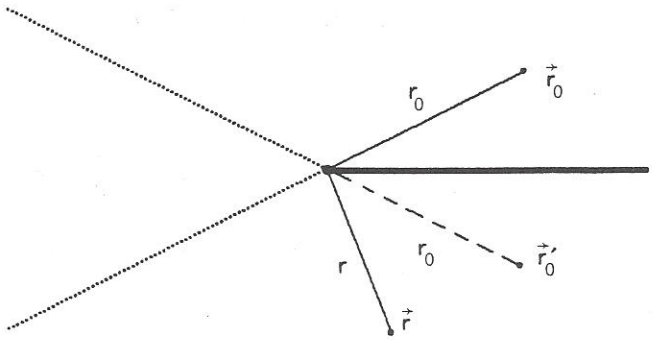

Figure 6a.

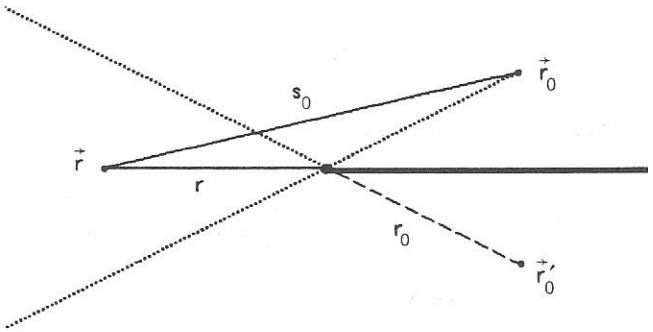

Figure 6b.

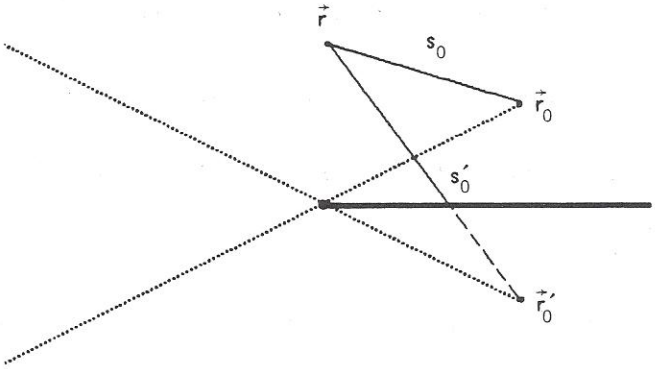

Figure 6c.

Figure 6. The locations of the source, image source, edge and observation points determine the minimum length direct paths ξ_d and ζ_d. (a) $\vec{r}$ is in Region I; (b) $\vec{r}$ is in Region II; and (c) $\vec{r}$ is in Region III.

$$\psi_{\pm} = \theta \mp \theta_0 - (\pi \pm \theta_0) \tag{4.6}$$

Let be the angles measured from the source shadow boundary (ψ_+) and from the shadow boundary of its image (ψ_-). Then, for instance, $\psi_+ < 0$ in the lit region of the source and $\psi_+ > 0$ in its shadow region. Defining the detour parameters

$$\Omega = (2k\rho)^{1/2} \sin(\psi_+/2) \tag{4.7}$$

$$\Omega' = (2k\rho')^{1/2} \sin(\psi_-/2) \tag{4.7'}$$

the half-plane solution in all cases is simply

$$U(\vec{r}) = \frac{1}{2}[W(s_0, \Omega) \mp W(s_0', \Omega')] \tag{4.8}$$

The detour parameters (4.7) and (4.7') are analogous to those introduced for the plane wave half-plane problem by Lee and Deschamps [13].

The distinction between the direct and indirect paths is emphasized by the solutions for cases 2 and 3. When the observation point is in the lit region of one of the sources, the direct propagator recovers the field incident from that source – the free-space propagator. In contrast, the propagator arising from the indirect paths clearly represents the diffraction process – the interaction of the incident field with the edge of the half-plane. This refines Sommerfeld's original conclusion [14, pp. 256-257] that the transition from one sheet of P_2 to the other constitutes the diffraction phenomena. It also reinforces the conclusion that the diffraction effects originate in the modification of the free-space path set by the presence of the half-plane.

5. ASYMPTOTIC CONSIDERATIONS

The standard GTD concepts of the direct and diffracted rays [3] are closely related to the direct and indirect path set effects. These connections are elucidated by considering the high frequency ($k \to \infty$) asymptotic approximations of the path-length forms of the PI expressions. They also reaffirm the physically appealing aspects of GTD: a generalized Fermat's principle and a localization of the relevant physical effects.

According to Keller's theory, the indirect (kinked) path $\vec{r}_0\sigma\vec{r}$ minimizes the action (1.3) in addition to the direct (straight line) path $\vec{r}_0\vec{r}$. Hence, for $\vec{r}$ in the lit region of the source the propagator should asymptotically be a combination of the contributions $\tilde{K}_d$ and $\tilde{K}_i$ from the neighborhoods of these two types of stationary paths:

$$K(\vec{r}, \vec{r}_0) = \int_{\Gamma} e^{\nu(S|\gamma)}\, D\gamma \;\sim\; \tilde{K}_d(\vec{r}, \vec{r}_0) + \tilde{K}_i(\vec{r}, \vec{r}_0) \tag{5.1}$$

Moreover, the edge is recognized as the fundamental source of the diffraction effects. To account for this, the minimum length indirect path is identified as the

diffracted ray and a diffraction coefficient χ_+ is introduced to represent the edge interaction. With the asymptotic form of the free-space propagator

$$K_F(\vec{r},\vec{r}_0) \sim g(ks_0) = \frac{e^{i(ks_0+\pi/4)}}{(8\pi k s_0)^{1/2}} \tag{5.2}$$

Keller assumes that

$$\tilde{K}_d(\vec{r},\vec{r}_0) = g(ks_0) \tag{5.3}$$

and

$$\tilde{K}_i(\vec{r},\vec{r}_0) = g(kr)\,\chi_+\,g(kr_0) \tag{5.4}$$

which corresponds to the Feynman diagram:

$K(\vec{r},\vec{r}_0) \quad \sim$  (5.5)

Direct Ray Diffracted Ray

The diffraction coefficient is obtained from the asymptotic form of the exact solution.

This asymptotic structure arises naturally from the path-length expressions. As above, let $\vec{r}$ be in the lit region of the source. The propagator

$$K(\vec{r},\vec{r}_0) = K_F(\vec{r},\vec{r}_0) - \frac{1}{4\pi}\int_{r+r_0}^{\infty} \frac{e^{\nu s}\,ds}{(s^2-s_0^2)^{1/2}} \tag{5.6}$$

The asymptotic form of the direct contributions obviously gives the geometrical optics field:

$$K_d(\vec{r},\vec{r}_0) = K_F(\vec{r},\vec{r}_0) \sim \tilde{K}_d(\vec{r},\vec{r}_0) \equiv g(ks_0) \tag{5.7}$$

The natural choice for the asymptotic approximation of the indirect paths term is an endpoint evaluation. Standard stationary phase arguments are not appropriate because the kinked minimum length indirect path $\vec{r}_0\sigma\vec{r}$ lies on the boundary of the indirect path set. For a general integral this approximation has the form

$$\int_a^{\infty} e^{\nu f(x,y)}\,B(x,y)\,dx \sim -\nu^{-1}e^{\nu f(a,y)}\,B(a,y)/\partial_x f(a,y)$$

The indirect path propagator then yields the diffracted field:

$$K_i(\vec{r},\vec{r}_0) \sim \tilde{K}_i(\vec{r},\vec{r}_0) = -\frac{e^{\nu s_{min}}}{4\pi ik\,(s_{min}^2 - s_0^2)^{1/2}} \equiv g(kr)\,\chi_+\,g(kr_0) \qquad (5.8)$$

The diffraction coefficients

$$\chi_\pm = \csc(\psi_\pm/2) \qquad (5.9)$$

χ_- being obtained in a similar fashion from the image source indirect propagator. Clearly the direct and diffracted ray concepts are included intrinsically in the path-length PI representation. Moreover, the special significance ascribed to the edge is incorporated succinctly in the indirect path definition.

6. HALF-PLANE PROPAGATOR SYMMETRY RELATION

Equations (4.2) and (4.4) yield the detour parameter symmetry relation:

$$W(s_0,0) = \frac{1}{2}[W(s_0,\eta) + W(s_0,-\eta)] \qquad (6.1)$$

or

$$K_F(\vec{r},\vec{r}_0) = \frac{1}{2}[W(s_0,\eta) + W(s_0,-\eta)] \qquad (6.1')$$

With it one immediately recovers, for example, the standard symmetry relation associated with the half-plane problem solution:

$$U(r,\theta) - U(r,2\pi-\theta) = \frac{1}{2}\Big\{[W(s_0,\Omega) - W(s_0',\Omega')] - [W(s_0',-\Omega') - W(s_0,-\Omega)]\Big\}$$
$$= W(s_0,0) - W(s_0',0) = K_F(\vec{r},\vec{r}_0) - K_F(\vec{r},\vec{r}_0{}') \qquad (6.2)$$

On the other hand, it will be demonstrated that symmetry relations mimicking (6.1) are satisfied by all of the canonical half-plane problem solution functions. Moreover, (6.1′) will be connected to an intrinsic property of the half-plane propagator on P_2. Several other interesting relations satisfied by the half-plane propagator are also revealed.

Consider the (two-dimensional) problem of a plane wave incident on the half-plane from the direction θ_0. The solution is generated from (4.8) by letting $r_0 \to \infty$ and multiplying it by $g^{-1}(kr)$. Setting the Fresnel function

$$F(x) = \frac{e^{-i\pi/4}}{\pi^{1/2}} \int_x^\infty e^{iu^2}\,du \qquad (6.3)$$

and the detour parameters $\Omega_0 = (2kr)^{1/2}\sin(\psi_+/2)$ and $\Omega_0' = (2kr)^{1/2}\sin(\psi_-/2)$, the total field is

$$U_P(\vec{r}) = \exp[-ikr\cos(\theta-\theta_0)]F(\Omega_0) \mp \exp[-ikr\cos(\theta+\theta_0)]F(\Omega_0') \qquad (6.4)$$

Subsequently, defining the function

$$W_p(\vec{r},\theta_0) = 2\exp[-ikr\cos(\theta-\theta_0)]\,F(\Omega_0)$$

and the plane wave

$$U_p^{inc}(\vec{r}) = \exp[-ikr\cos(\theta-\theta_0)]$$

the solution (6.4) becomes

$$U_p(\vec{r}) = \frac{1}{2}[W_p(\vec{r},\theta_0) \mp W_p(\vec{r},-\theta_0)] \tag{6.4'}$$

and the symmetry relation

$$W_p(\vec{r},0) = \frac{1}{2}[W_p(\vec{r},\theta_0) + W_p(\vec{r},-\theta_0)] = U_p^{inc}(\vec{r}) \tag{6.5}$$

results from the Fresnel function properties [13]: $F(0) = 1/2$ and $F(x)+F(-x) = 1$. These relations remain valid in the corresponding three-dimensional, oblique incidence case when the substitutions $k \to k\sin\beta$, $r \to r\sin\beta$, and $W_p \to W_p\exp(ikr\,\cos^2\beta)$ are made, the plane wave being incident at an angle β with respect to the edge.

Similar considerations apply to the three-dimensional problem of a spherical wave incident on the half-plane from a point source. The incident field

$$K_F(\vec{r},\vec{r}_0) = \frac{e^{\nu|\vec{r}-\vec{r}_0|}}{4\pi|\vec{r}-\vec{r}_0|} \tag{6.6}$$

where $\vec{r}_0 = (r_0,\theta_0,z_0)$ and $\vec{r} = (r,\theta,z)$ so that the (straight-line) distance

$$|\vec{r}-\vec{r}_0| = s_0 = [r^2 + r_0^2 - 2rr_0\cos(\theta-\theta_0) + (z-z_0)^2]^{1/2}$$

Because [22, Eq. 5.4.12d]

$$\frac{e^{\nu s_0}}{4\pi s_0} = \frac{i}{8\pi}\int_{-\infty}^{\infty} H_0^{(1)}[(k^2-\zeta^2)^{1/2}R(\theta-\theta_0)]e^{i\zeta(z-z_0)}\,d\zeta \tag{6.7}$$

where $R(\theta-\theta_0) = [r^2 + r_0^2 - 2rr_0\cos(\theta-\theta_0)]^{1/2}$ and ζ is the wave vector component along the z-axis, the total field may be derived from the line source case by replacing k with $(k^2-\zeta^2)^{1/2}$ in that solution and by applying the operator $(i/8\pi)\int_{-\infty}^{\infty} d\zeta\exp[i\zeta(z-z_0)]$ to it. On the other hand, because the free-space propagator [21, 11.7.37]

$$\frac{e^{\nu s_0}}{4\pi s_0} = \frac{\nu}{4\pi}\int_{-\infty}^{\infty}\frac{H_1^{(1)}(\tau^2+ks_0)\,d\tau}{(\tau^2+ks_0)^{1/2}} = \frac{\nu}{4\pi}\int_{s_0}^{\infty}\frac{H_1^{(1)}(ks)\,ds}{(s^2-s_0^2)^{1/2}} \tag{6.7'}$$

the path-length/detour parameter approach to the line source problem is directly applicable. In particular, let $\vec{\sigma}$ be the point on the edge where the straight lines $\vec{r}_0\vec{\sigma}$ and $\vec{\sigma}\vec{r}$ both make an angle β with respect to the edge and let $\rho_1 = |\vec{\sigma} - \vec{r}_0|$ and $\rho_2 = |\vec{r} - \vec{\sigma}|$ be the distances associated with those paths. The minimum length indirect path is the kinked path $\vec{r}_0\vec{\sigma}\vec{r}$ and has the length $\rho_1 + \rho_2 = [(r + r_0)^2 + (z - z_0)^2]^{1/2}$. The corresponding detour parameter is

$$\Omega_s = (2k\rho_s)^{1/2} \sin\beta \, \sin(\psi_+/2) \tag{6.8}$$

where $\rho_s = 2\rho_1\rho_2/(\rho_1 + \rho_2 + s_0)$. The image source detour parameter Ω_s' is simply (6.8) with the substitutions $\psi_+ \to \psi_-$ and $s_0 \to s_0'$. Introducing the function

$$W_s(\alpha, \beta) = \frac{\nu}{2\pi} \int_\beta^\infty \frac{H_1^{(1)}(\tau^2 + k\alpha)\, d\tau}{(\tau^2 + 2k\alpha)^{1/2}} \tag{6.9}$$

the detour parameter form of the solution is

$$U(\vec{r}) = \frac{1}{2}[W_s(s_0, \Omega_s) \mp W_s(s_0', \Omega_s')] \tag{6.10}$$

and the symmetry relation

$$W_s(s_0, 0) = \frac{1}{2}[W_s(s_0, \Omega) + W_s(s_0', \Omega')] = K_F(\vec{r}, \vec{r}_0) \tag{6.11}$$

is obtained. Path-length versions of (6.10) for the various source-edge-observation point configurations are obviously available and have the same structure as the line source case expressions.

Returning now to the line source case, consider the detour parameter representation of the source propagator:

$$K(\vec{r}, \vec{r}_0) = \frac{1}{2} W(s_0, \Omega) \tag{6.12}$$

Since the substitution $\theta \to \theta + 2\pi$ causes $\Omega \to -\Omega$, the relation (6.1) gives the symmetry condition:

$$K_F(r, \theta; \vec{r}_0) = K(r, \theta; \vec{r}_0) + K(r, \theta + 2\pi; \vec{r}_0) \tag{6.13}$$

From a P_2-space point of view, this means the sum of the propagators at the preimages of the observation point equals equivalently the incident field or the free-space propagator. This relation was recognized by Sommerfeld [14] and Carslaw [23,24] from their contour integral representations of the solution. Carslaw also established this property for the solutions of the corresponding heat and potential problems. The relation (6.13) is an intrinsic property of the P_2-space solutions of half-plane problems.

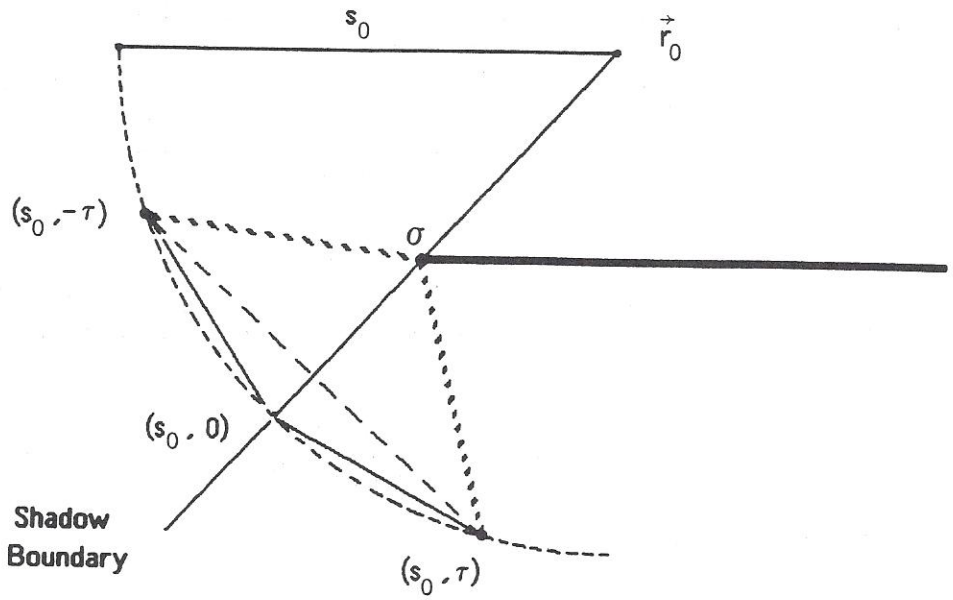

Figure 7. The propagators from $\vec{r}_0$ to a particular configuration of observation points $\vec{b}$, and $\vec{b}_\pm$ are related by (6.15).

Equations (6.1) and (6.13) are actually manifestations of a more fundamental concept. Evaluating (6.13) at a point $\vec{r} = (w, 0)$ on the "branch cut" Σ, one obtains

$$\Phi_-(w) = T(w)\,\Phi_+(w) + F(w)$$

where $T(w) = -1$, $\Phi_+(w) = K(w, 0; \vec{r}_0)$, $\Phi_-(w) = K(w, 2\pi; \vec{r}_0)$, and $F(w) = K_F(w, 0; \vec{r}_0)$. This transition condition relates the values of K on two sides of the branch cut. In fact, it represents an inhomogeneous Riemann-Hilbert problem [4, 25, 26], T being its coefficient and F its free term. The propagator $K(\vec{r}, \vec{r}_0)$ is its solution; the function $W(s_0, \Omega)$ is the solution to the related Riemann-Hilbert problem whose free-term is $2F$.

In this context, (6.13) rewritten as

$$K(r, \theta + 2\pi; \vec{r}_0) = -K(r, \theta; \vec{r}_0) + K_F(r, \theta; \vec{r}_0) \qquad (6.13')$$

and the relation

$$K(r, \theta + 4\pi; \vec{r}_0) = +K(r, \theta; \vec{r}_0) \qquad (6.14)$$

which follows directly from (6.12) or (6.13), describe how the different branches of K fit together as one loops about the edge. One observes that a single loop about σ involves the transition (6.13') and a double loop returns the original function. These results recover the monodromy group $\{e^{in\pi}; n = 0, 1\}$ which was introduced in a related context in Section 3. The coefficient $T(w) = -1$ is also

characteristic of the square root behavior of the solution near the edge σ.

The symmetry relation (6.1) has several other interesting ramifications. Referring to Fig. 7, the point $\vec{b} = (r, \pi + \theta_0)$ lies on the source shadow boundary and the points $\vec{b}_\pm = (r, \pi + \theta_0 \pm \phi)$ are symmetrically located with respect to it, being equidistant from the point $\vec{b}$ and equidistant from σ. Moreover, all three points lie on the circle of radius s_0 centered at $\vec{r}_0$. Equation (6.1) indicates that the propagator to a shadow boundary point $\vec{b}$ is the average of the propagators to any pair of points $\vec{b}_\pm$:

$$K(r, \theta_0 + \pi; \vec{r}_0) = \frac{1}{2}[K(r, \theta_0 + \pi - \phi; \vec{r}_0) + K(r, \theta_0 + \pi + \phi; \vec{r}_0)] \qquad (6.15)$$

The single detour parameter expression (6.12) represents the solution to many source-edge-observation point configurations. In particular, consider an ellipse whose focal points are $\vec{r}_0$ and $\vec{r}$. Every configuration for which σ lies on this ellipse and the half-plane separates the ellipse into two regions, each containing either $\vec{r}_0$ or $\vec{r}$ but not both, has the same minimum detour parameter $\Omega = \eta > 0$. Two examples of this case are shown in Fig. 8a. Consequently, all of these configurations are represented by a single point on the positive Ω-axis shown in Fig. 9 and support the propagator $\frac{1}{2}W(s_0, \eta)$. Similarly, any configuration in which σ lies on the ellipse but the half-plane does not separate $\vec{r}_0$ and $\vec{r}$ has the minimum detour parameter $\Omega = -\eta < 0$ and supports the propagator $\frac{1}{2}W(s_0, -\eta)$. They are represented by the point $-\eta$ on the Ω-axis in Fig. 9. Examples of these cases are given in Fig. 8b. Finally, the configurations for which the minimum detour parameter $\Omega = 0$ have σ lying on the straight segment connecting $\vec{r}_0$ to $\vec{r}$ and support half of the free-space propagator $\frac{1}{2}W(s_0, 0)$. Examples of these cases are given in Fig. 8c. They are represented by the point $\eta = 0$ in Fig. 9. These results suggest that the propagator $K(\vec{r}, \vec{r}_0)$ may be viewed as resulting from sums over paths with particular detour parameter sets. Setting $\Phi(\eta) \equiv \frac{1}{2}W(s_0, \eta)$, the propagators associated with Figs. 8a, 8b, and 8c and with free-space are, respectively, $\Phi(\eta)$, $\Phi(-\eta)$, $\Phi(0)$, and $\Phi(-\infty)$. The corresponding detour parameter intervals are $[\eta, \infty[$; $[-\eta, \infty[$; $[0, \infty[$; and $]-\infty, \infty[$. The minimum detour is fixed by the given configuration, and the half-plane suppresses contributions to the PI from paths whose detours are less than that minimum. In this context, the symmetry relation (6.1) becomes

$$\Phi(-\infty) = \Phi(\eta) + \Phi(-\eta) = 2\Phi(0)$$

or

$$\Phi(\eta) - \Phi(0) = \Phi(-\eta) - \Phi(0) \qquad (6.16)$$

which indicates the sum over paths with detour parameters in the interval $[0, \eta]$ equals the sum over those in $[-\eta, 0]$. Furthermore, it is ascertained that the difference between the propagators associated with Figs. 8a and 8b is

$$\Phi(-\eta) - \Phi(\eta) = 2[\Phi(0) - \Phi(\eta)] \qquad (6.17)$$

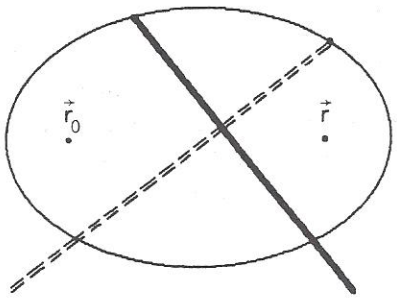

Figure 8a.

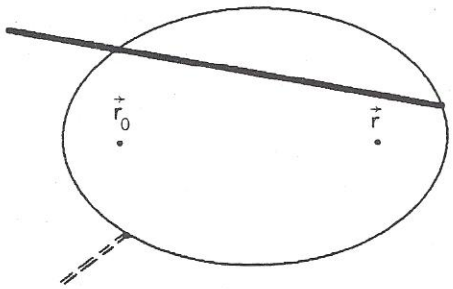

Figure 8b.

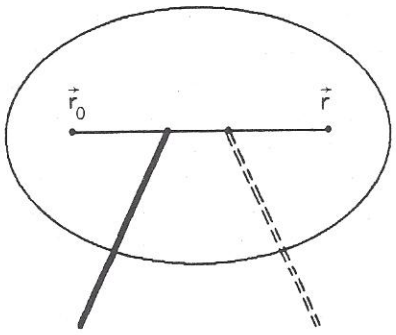

Figure 8c.

Figure 8. Each detour parameter expression encompasses a large variety of possible configurations. Examples are given where the detour parameter (a) $\Omega > 0$; (b) $\Omega < 0$; and (c) $\Omega = 0$.

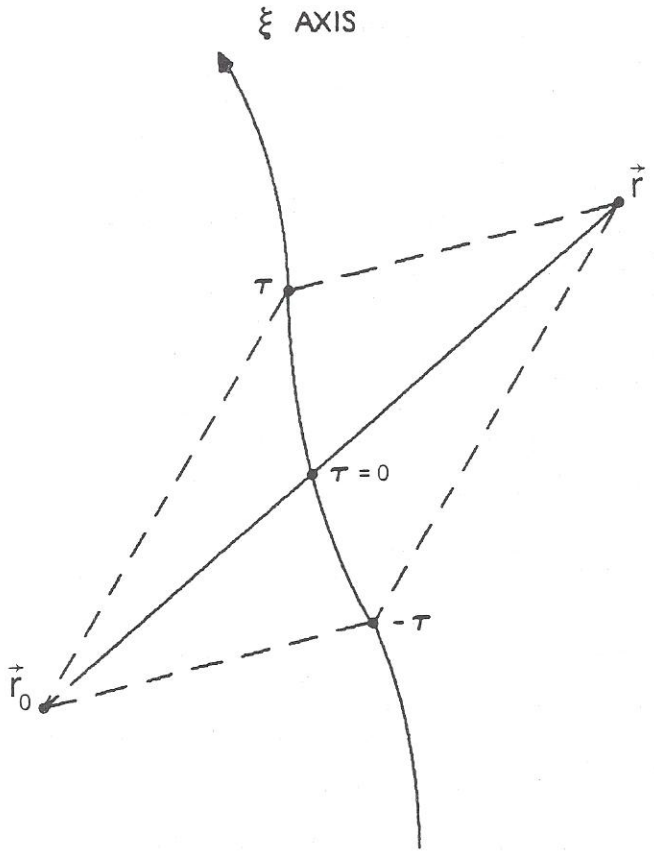

Figure 9. The half-plane path sets can be organized from a detour parameter point of view.

The difference results from all of those paths whose detours are in the interval $[0, \eta]$; i.e., the paths contained in the ellipse.

Similar conclusions may be drawn for the related two- and three- dimensional versions of the electromagnetic half-plane problem. They also pertain to the corresponding heat and potential problems.

ACKNOWLEDGMENTS

The author would like to express his deepest appreciation to Professor G. A. Deschamps for his invaluable comments and suggestions as this paper evolved. This work was supported in part by the grant NSF-ENG-77-20820 and by the Lawrence Livermore National Laboratory under the auspices of the U.S. Department of Energy under contract W-7405-ENG-48.

The Editor thanks E. V. Jull, S. W. Lee, A. Sezginer and one anonymous Reviewer for reviewing this paper.

REFERENCES

1. Feynman, R. P., and A. R. Hibbs, *Quantum Mechanics and Path Integrals*, McGraw-Hill, NY, 1965.
2. Ziolkowski, R. W., *J. Math. Phys.*, Vol. 27, 2271, 1986.
3. Keller, J. B., *J. Opt. Soc. Am.*, Vol. 52, 116, 1962.
4. Gakhov, F. D., *Boundary Value Problems*, Pergammon Press, NY, 1966.
5. Lee, S. W., *J. Math. Phys.*, Vol. 19, 1414, 1978.
6. Schulman, L. S., *The Wave-Particle Dualism*, proceedings of a conference in honor of L. de Broglie, Perugia, 1982, S. Diner, D. Fargue, G. Lochak, and F. Selleri, Eds., Reidel, 253–272, 1984.
7. Schulman, L. S., *Phys. Rev. Lett.*, Vol. 49 (9), 599, 1982.
8. Wiegel, F. W., and J. Boersma, *Physica*, Vol. 122A, 325, 1983.
9. Dowker, J. S., *J. Phys. A: Math. Gen.*, Vol. 10, 115, 1977.
10. DeWitt-Morette, C., S. G. Low, L. S. Schulman, and A. Y. Shiekh, *Found. Phys.*, Vol. 16, 311, 1986.
11. Crandall, R. E., *J. Phys. A: Math. Gen.*, Vol. 16, 513, 1983.
12. Gradshteyn, I. S., and I. M. Ryzhik, *Table of Integrals, Series, and Products*, Academic Press, NY, 1965.
13. Lee, S. W., and G. A. Deschamps, *IEEE Trans. Antennas Propagat.*, Vol. AP–24, 25, 1976.
14. Sommerfeld, A., *Optics*, Academic Press, NY, Sec. 38, 1954.
15. Chinn, W. G., and N. E. Steenrod, *First Concepts of Topology*, Random House, NY, 1966.
16. Dowker, J. S., *J. Phys. A.: Gen. Phys.*, Vol. 5, 936, 1972.
17. Laidlaw, M. G. G., and C. Morette-DeWitt, *Phys. Rev. D*, Vol. 3, 1375, 1971.
18. Schulman, L., *Phys. Rev.*, Vol. 176, 1558, 1968.
19. Schulman, L., *J. Math. Phys.*, Vol. 12, 304, 1971.
20. Schulman, L., *Functional Integration and Its Applications*, Claredon Press, Oxford, Chapter 12, 1975.
21. Born, M., and E. Wolf, *Principles of Optics*, The Macmillan Co., NY, second edition, 1964.
22. Felsen, L. B., and N. Marcuvitz, *Radiation and Scattering of Waves*, Prentice-Hall, Inc., Englewood Cliffs, NJ, 1973.
23. Carslaw, H. S., *Proc. London Math. Soc.*, (Ser. 2), Vol. 30, 121, 1899.
24. Carslaw, H. S., *Proc. London Math. Soc.*, (Ser. 2), Vol. 8, 365, 1910.
25. Zverovich, E. I., *Russian Math. Surveys*, Vol. 26, 117, 1971.
26. Ziolkowski, R. W., *SIAM J. Math. Anal.*, Vol. 16, 358, 1985.

Richard W. Ziolkowski (ScB'74–M'75–PhD'80) received the Sc.B. degree in physics with honors from Brown University in 1974, the M.S. and Ph.D. degree from the University of Illinois at Urbana-Champaign in 1975 and 1980, respectively. He joined the Engineering Research Division at the Lawrence Livermore National Laboratory in 1981 and is currently the Computational Electronics and Electromagnetics Thrust Area Leader for the Engineering Department. His research interests include the application of new mathematical methods to linear and nonlinear problems dealing with the interaction of electromagnetic waves with scattering objects, plasmas, and dielectric materials. Dr. Ziolkowski is a member of IEEE, URSI Commission B, Sigma Xi, Phi Kappa Phi, and American Physical Societies.